23rd ABCM International Congress of Mechanical Engineering
December 6-11, 2015, Rio de Janeiro, RJ, Brazil

EVALUATION OF PIV INTERROGATION STRATEGY IN THE INVESTIGATION OF THE LIQUID PHASE VELOCITY IN A BUBBLE COLUMN SECTION

Rodrigo de Lima Amaral
University of Campinas, School of Chemical Engineering, Albert Einstein ave., 500 – Zip Code: 13083-852, Campinas-SP, Brazil.
rlamaral@feq.unicamp.br
Diana Isabel Sánchez Forero
sanchezd@feq.unicamp.br
Guilherme José de Castilho
guilhermejc@feq.unicamp.br
Sávio Souza Venâncio Vianna
savio@feq.unicamp.br
Milton Mori
mori@feq.unicamp.br

Abstract. *Particle image velocimetry (PIV) has become attractive in the investigation of several flow. The processing of PIV images requires a careful selection of interrogation parameters in order to determine the highest correlation peak resulting in a calculation more precise of velocity. This work aims to assess the best PIV interrogation strategy (size and overlap of the interrogation windows) in the investigation of the liquid phase velocity in a bubble column section using the standard cross-correlation. The size and overlap of the interrogation windows were analyzed using correlation coefficient and signal-to-noise ratio (SNR) as quality parameters. Experimental tests were carried out in a water-air system in a cylindrical acrylic column of 1 m high and 141 mm diameter. Rhodamine B as tracer particle, a CCD camera (1376 x 1040 pixels and 12 bits) and a high-pass filter (560 nm) were used. The resolution of the image system was 12 pixels/mm and the investigated area was located from 55.2 cm of the gas distributor. The Nd:YAG (200 mJ) laser system, a lens with focal length of - 10 and a box with slit were used to produce a top-hat profile of light. The results show that different interrogation strategy is required for each gas flow rate in order to increase the correlation coefficient and signal-to-noise ratio.*

Keywords: *PIV Interrogation; Correlation; Bubble Column, Two-Phase Flow, Signal-to-Noise Ratio*

1. INTRODUCTION

Particle Image Velocimetry (PIV) has become a very attractive technique in experimental analysis of multiphase flows found in bubble columns. PIV is not an intrusive measurement technique and it uses the displacement pattern of the tracer particles present in the flow registered by a CCD or CMOS sensor to extract the fluid velocity distribution. An essential feature of the PIV methodology is the automation and quantification of the two-dimensional image displacement $\mathbf{X_p}$ in a small region called the interrogation window and can be quickly measured over the entire field of view. This step of the PIV analysis is referred to as image interrogation. After the interrogation, the displacement field is validated by the application of several criteria developed in order to identify invalid displacement vectors. These invalid vectors are image displacements that not represent the movement of one particle or group of particles (Raffel *et al*., 2007; Adrian and Westerweel, 2011).

The evaluation of particle images depends on the way that these images were recorded. One possibility of recording is known as double-frame/single-exposure, in which the light scattered by particles in the first and second illumination are recorded in different frames. Using this mode, the images can be analyzing by cross-correlation. In the case of field with non-homogeneous image or with strong displacement gradient, the standard method of cross-correlation presents a reduction of the displacement detection of the correlation peak and may be less appropriate. For these situations other PIV interrogation strategies can produce better results than standard methods as ensemble or pyramid correlation (Adrian and Westerweel, 2011).

This work aims to assess the best PIV interrogation strategy (size and overlap of the interrogation windows using standard correlation method) in the investigation of the liquid phase velocity in a bubble column section using Fluorescent PIV.

2. PIV CROSS-CORRELATION

The frame is first divided into smaller sub-regions called interrogation windows containing local distributions of light intensity (Fig. 1a). The two light intensities I_1 (i, j) and I_2 (i, j) within an interrogation window to the time t and t + dt respectively in the i-th and j-th pixels are then correlated. For cross-correlation, the interrogation windows do not have to necessarily be located at the same position of the PIV recording, in order to improve the image displacement detection. Two investigation areas separated by a sufficiently small time interval used for the statistical evaluation define the measuring volume. The distribution of tracer particles is described in terms of an image pattern for purposes of PIV image analysis. The particle images show the instantaneous positions of the tracer particles as light intensity peaks. The two images are light intensity distributions with the second exposure displaced in relation to the first (Fig. 1a) for a sufficiently short time interval (dt) (Raffel *et al*., 2007; Adrian and Westerweel, 2011).

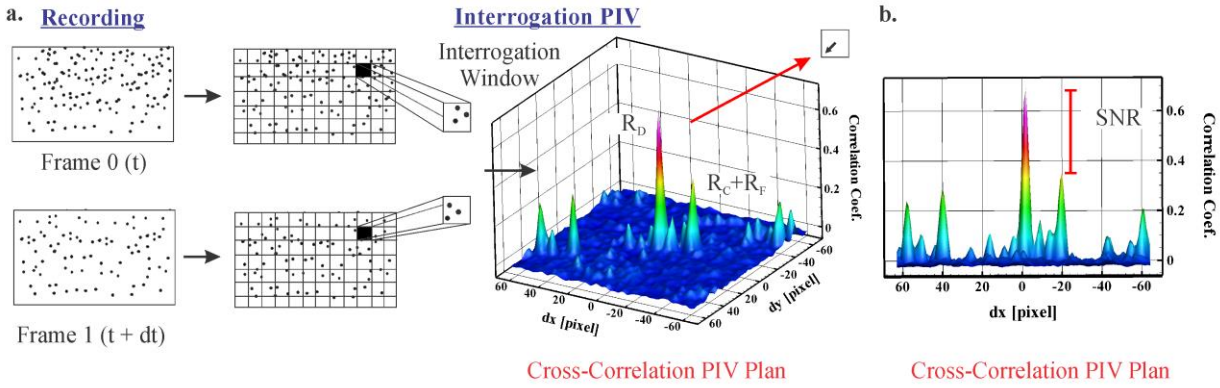

Figure 1. (a) Recording and PIV interrogation. (b) Definition of Signal-to-Noise Ratio (SNR).

The sum of products of all light intensities that overlap the pixels in each spatial displacement (dx, dy) returns the correlation value map C (dx, dy), Eq. 1, that is essentially a measure of the correspondence degree between the two samples for a given spatial displacement. A correlation map is formed by applying Eq. 1 for a spatial displacement range. In Eq.1 and Eq. 3, $M_{I1} \times M_{I2}$ is the interrogation area size, μ_{I1} is the average of I_1 and μ_{I2} is the average of I_2. In Eq. 2, the highest peak in the correlation map is c (dx, dy), and it represents the most probable displacement within each interrogation window. Knowing the separation time dt, the velocity vector field can be obtained. The PIV cross-correlation plan (Fig. 1a) represents the probability distribution of all possible particle image displacement patterns between consecutive frames and it may be written by Eq. 4. The PIV cross-correlation plan presents a combination of effects of various sources of errors that govern the accuracy of the particle image displacement pattern. In Eq. 4, R_D is the correlation peak of the particle images displacement, R_C is the average background correlation and R_F is the correlation due to the random movement of particle images in the interrogation window (Raffel *et al*., 2007; Adrian and Westerweel, 2011). A practical measure of cross-correlation quality is the signal-to-noise ratio (SNR), which is defined as the ratio of the highest correlation peak and the second highest peak (Fig. 1b). Numerical investigations show that a correlation coefficient of 0.5 and an SNR of 2.0 are ideal to avoid errors in the field vector (XUE *et al*., 2013).

$$C(dx,dy)=\sum_{i=0}^{M}\sum_{j=0}^{N}\left[I_1(i,j)-\mu_{I_1}\right]\left[I_2(i+dx,j+dy)-\mu_{I_2}\right] \quad (1)$$

$$c(dx,dy)=\frac{C(dx,dy)}{\sqrt{\sigma_1}\sqrt{\sigma_2}} \quad (2)$$

where $$\sigma(x,y)=\sum_{i=0}^{M_{I2}}\sum_{j=0}^{M_{I1}}\left[I\ (i,j)-\mu_I\ \right]^2. \quad (3)$$

$$R(s,t)=R_C(s,t)+R_F(s,t)+R_D(s,t) \quad (4)$$

3. EXPERIMENTAL

The experimental tests were carried out using an acrylic column with a height of 1 m and diameter of 14.5 cm (Fig 2a). Water and air (25°C) were used as liquid and gaseous phases, respectively. The liquid height from the gas distributor was 80 cm and a box filled with water (25°C) was used in the investigation region to decrease the distortion caused by the column curvature. The size of the field of view (FoV) was 14.5 x 13 cm and it was located 55.2 cm from the gas distributor (Fig. 2b). The air distributor has 21 holes of 1 mm diameter each and it has a square arrangement (Fig. 2c). Three gas flow rate were used: 5, 20 and 40 L/min.

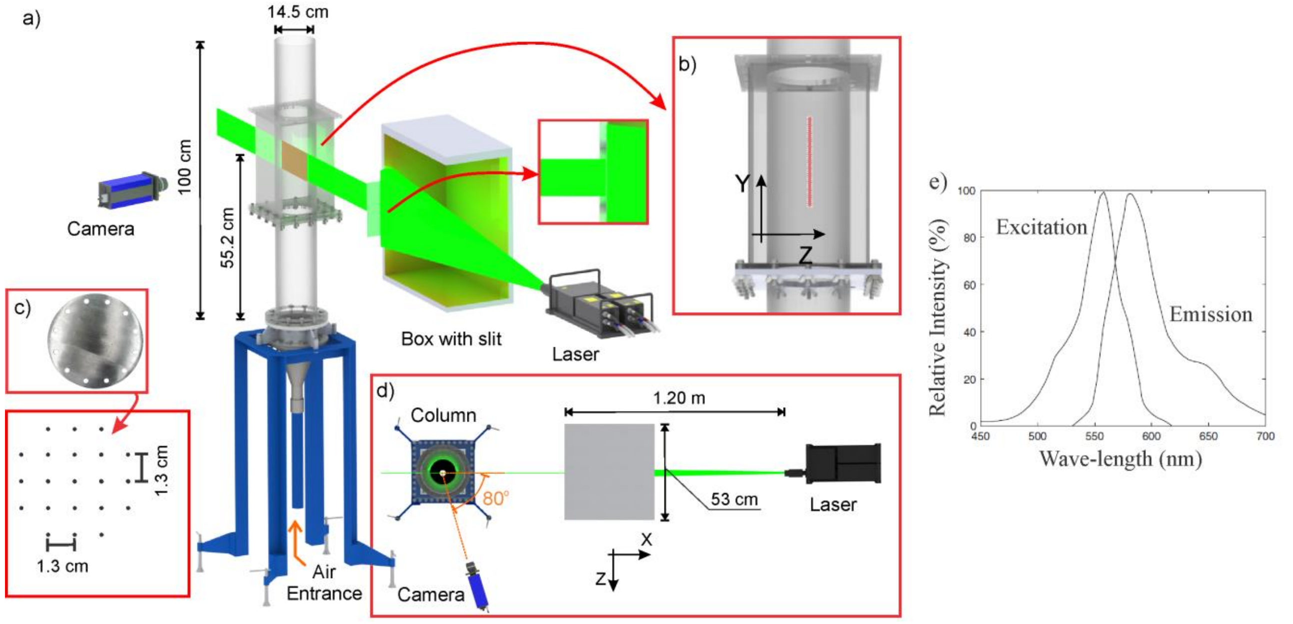

Figure 2 - (a) Column, PIV system and box with slit. (b) Field of View (FoV). (c) Air distributor with 21 holes. (d) PIV system arrangement in the column. (e) Excitation and emission spectrum of the Rhodamine B (Adapted from Wilson *et al*., 1986).

The PIV system used was developed by LaVision and it has a CCD sensor (1376 x 1040 pixels) with maximum frequency of 30 Hz and a Nd:YAG (200 mJ/pulse and $\lambda =$ 532 nm) laser system with maximum frequency of 5 Hz. The cameras and the laser system can be controlled with a programmable time unit (PTU) by Davis 8.2 software with a recording frequency of 5 Hz. The CCD camera was placed at 80 degrees from the light plan in an angular configuration satisfying the Scheimpflug condition (Fig. 2d). This condition ensures the focus throughout the field of view. An objective lens with focal distance of 60 mm (F/2.8D), Rhodamine-B as trace particle and a high-pass filter on the camera that allows only the passage of emitted light by tracer (λ = 620 nm, Fig. 2f) were used as the PIV technique complements (Fluorescent PIV). Besides using an acrylic box with water in the investigated area, a calibration procedure was performed in order to correct the image distortion caused by the column curvature using a 3rd order polynomial fit (mapping function) resulting in an average calibration error of 0.952 pixel. The laser beam was expanded using a cylindrical negative lens and a box with a slit of 1 mm thickness located 1.20 m from laser (Fig. 2d) was used in order to produce a light plan with a homogeneous intensity profile (top-hat). The resolution of the imaging system was 12 pixels/mm. 4000 pairs of images were recorded with a frequency of 4.2 Hz and the inter-frame time was 1000 µs, producing a particle image maximum displacement of 15 - 20 pixels. The RMS (Root Mean Square) and SSM (Subtract Sliding Minimum) filter of 3x3 pixels were applied sequentially in the recorded images. A pixel intensity lower than 10 counts was defined as 0 counts and an upper limit of 50 counts was used in order to improve the image contrast.

The evaluation of multiple steps was used in the PIV correlation with decreasing interrogation window using Adaptive PIV method (Wieneke and Pfeiffer, 2010). This method changes the size and shape of the interrogation window automatically according to the particle image density and flow gradients with the aim to increase the correlation coefficient and SNR. The overlap of the interrogation window with its neighborhood was used in order to increase the spatial resolution of the vector field. Moreover, the initial and final size of the interrogation window was defined 2 and 3 passes to ensure the convergence in determining the particle image displacement. The interrogation strategies (size and overlap of the interrogation windows) analyzed using the standard cross-correlation are shown in Tab. 1.

The mapping function obtained in the calibration procedure and the particle image displacement information of the first step was applied to the image reconstruction using a bicubic interpolation (Scarano and Riethmuller, 2000). An estimator of three points and a Gaussian function to the peak fit was used in the peak detectability.

The distributions of the time-averaged correlation coefficient, SNR and uncertainty estimated by Wieneke (2014) method were used as quality parameters of the interrogation strategy analyzed. The distributions of the time-averaged velocity (modulus and components) were compared with the measurements obtained by the ensemble correlation (PIV sum of correlation) method (Meinhart *et al*., 2000).

Table 1 – Interrogation strategies (size and overlap of the interrogation windows) analyzed using the standard cross-correlation.

Exp	Flow rate [L/min]	Laser power (%)	Interrogation Window Size (Pixel)		Overlap of Interrogation Window (%)		Label
			Initial	Final	Initial	Final	
1	5	20	512	256	25	50	256p 50%
2			512	256	50	75	256p 75%
3			256	128	25	50	128p 50%
4			256	128	50	75	128p 75%
5			128	96	25	50	96p 50%
6			128	96	50	75	96p 75%
7			96	64	25	50	64p 50%
8			96	64	50	75	64p 75%
9	20	35	512	256	25	50	256p 50%
10			512	256	50	75	256p 75%
11			256	128	25	50	128p 50%
12			256	128	50	75	128p 75%
13			128	96	25	50	96p 50%
14			128	96	50	75	96p 75%
15			96	64	25	50	64p 50%
16			96	64	50	75	64p 75%
17	40	35	512	256	25	50	256p 50%
18			512	256	50	75	256p 75%
19			256	128	25	50	128p 50%
20			256	128	50	75	128p 75%
21			128	96	25	50	96p 50%
22			128	96	50	75	96p 75%
23			96	64	25	50	64p 50%
24			96	64	50	75	64p 75%

4. RESULTS AND DISCUSSIONS

Figure 3 shows the distribution of the correlation coefficient, SNR and of the vector field without and with PIV post processing for an instantaneous image (image 937) using the interrogation strategy 256p 75% at a flow rate of 5 L/min. It is noted that at left side of the column ($-1 < r/R < 0$) there are regions in which the correlation coefficient is less than 0.3 (Fig. 3a) and the SNR near 2 (Fig. 3b). In these regions, the measurement quality is smaller and false vectors appear in the velocity field without PIV post processing (Fig. 3c). In good conditions, the number of invalid vectors is less than a few percent making the data validation by comparison with the displacement of neighborhood fairly easy. In Fig. 3d, regions with correlation coefficient lower than 0.5 had their vectors deleted using the post processing filter developed by Westerweel and Scarano (2005) to the substitution of the vectors. The distribution of the uncertainty estimated by Wieneke (2014) method is shown in Fig. 3e and 3f to Vx and Vy, respectively. The areas not illuminated by the laser light (Fig. 4) may be an explanation for the appearance of regions with low correlation coefficients, making the uncertainty of Vx and Vy higher on the left side of the column. The presence of bubbles in the column center difficults the illumination of the cross area even with the use of filters in the image preprocessing.

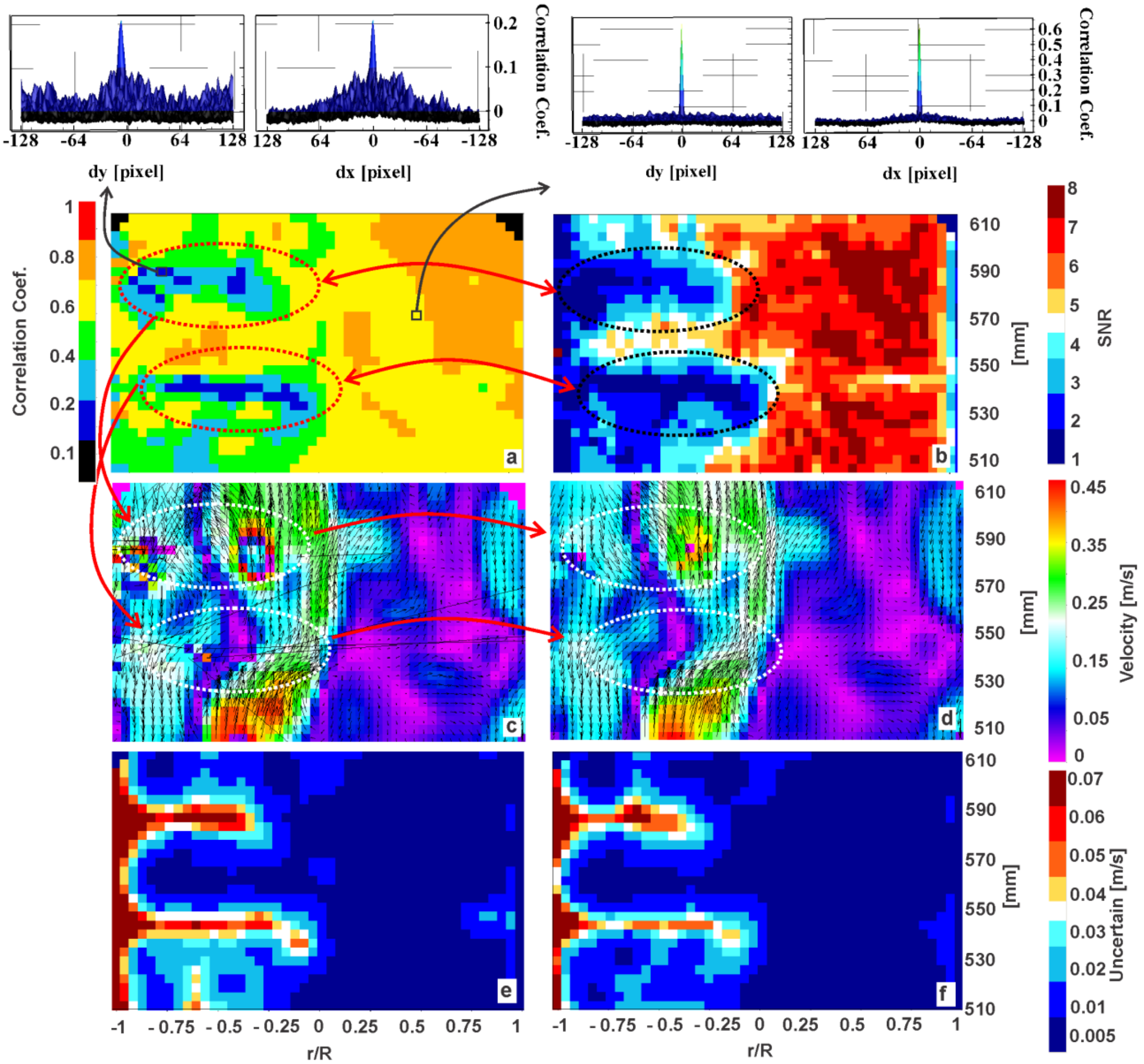

Figure 3 – Distributions of (a) correlation coefficient and (b) SNR. Vector field (c) without and (d) with PIV post processing for an instantaneous image (image 937) using the interrogation strategy 256p 75% at a flow rate of 5 L/min. Distributions of uncertainty of (e) Vx and (f) Vy estimated by Wieneke (2014) method.

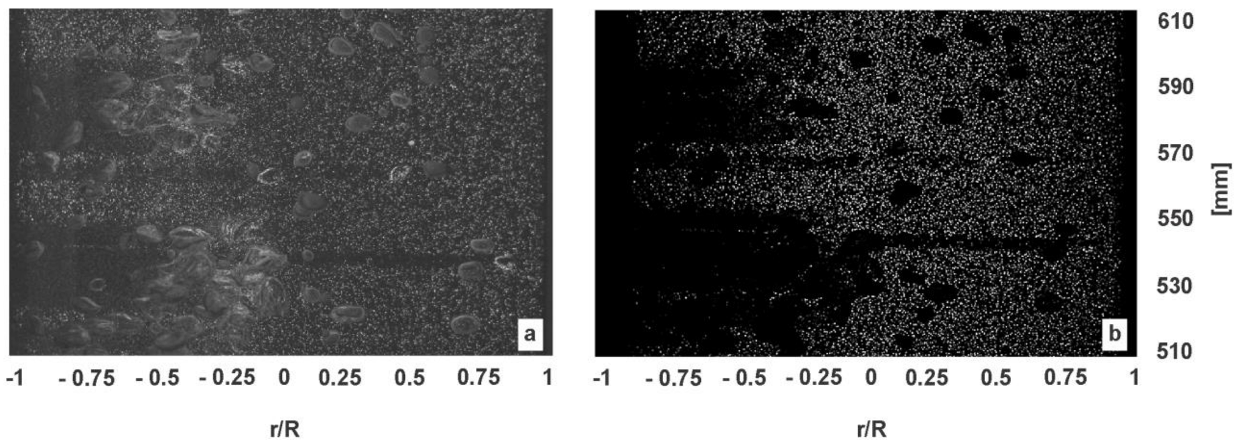

Figure 4. (a) Image 937 raw and (b) preprocessed of frame 0 used to calculate the fields of the Fig. 3.

Figure 5 shows the distribution of time-averaged correlation coefficient, SNR and uncertainty of V, Vx and Vy measurements across the radius for different interrogation strategies and flows of 5, 20 and 40 L/min at 55.2 cm from column distributor. One can see that both distributions of time-averaged correlation coefficient and SNR decrease with increasing gas flow rate and with the final size of the interrogation window.

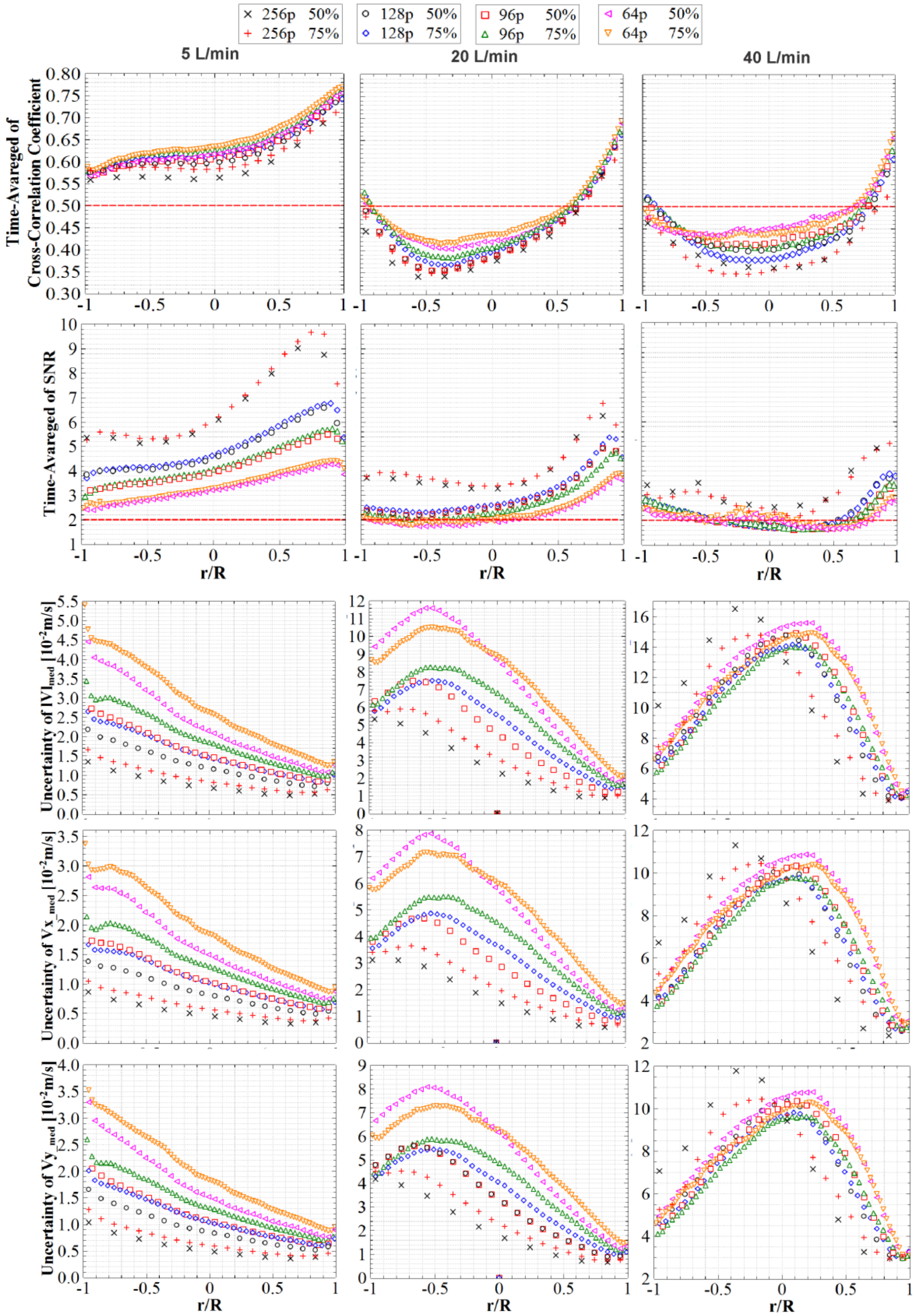

Figure 5. Distributions of time-averaged of correlation coefficient and SNR; uncertainty of V, Vx and Vy measurements across the radius for different interrogation strategies and flows of 5, 20 and 40 L/min

The effect on correlation can be explained by the velocity gradients in the field of view. The identification of the flow pattern on the correlation becomes better when the interrogation window size decreases. The effect on SNR can be explained by the presence of a few pairs of correlated particle images when the interrogation window size decreases. According to simulations performed by Keane and Adrian (1992), at least 5 pairs of correlated particle images are needed to have a reliable velocity vector. Due to the presence of bubbles which causes a non-homogeneous distribution of the laser light intensity in the field of view, it is observed that for the flow rate of 5 L/min the distribution of the time-averaged of correlation coefficient decreases from r/R = 1 to -1. Decrease of correlation coefficients in the column center are observed for flow rates of 20 and 40 L/min. This fact can be explained or by the presence of bubbles in front of the field of view, which compromises the recording of the particle images on the CCD sensor. The distributions of time-averaged uncertainty of V, Vx and Vy increase with increasing flow and decreasing of interrogation window size. It is also noticed that the distributions of time-averaged uncertainty increases from r/R = -1 to 1 at 5 L/min and 20 L/min with a maximum at r/R = - 0.5. In the case of 40 L/min, there is an increase in the column center. The correlation coefficient, SNR and uncertainty not presented the same behavior. The Wieneke (2014) method to estimate the uncertainty of PIV measurements mainly considers the peak shape and not the correlation coefficient or SNR. This method is limited due to the out-of-plane movement of particles on the images correlation.

Figure 6 shows the distributions of time-averaged V, Vx and Vy along the radius and for flow rates of 5, 20 and 40 L/min. The experiments presented in Tab.1 were carried out using standard cross-correlation and then compared with the average values of velocity (lines in Fig. 6) obtained by the ensemble correlation approach (PIV sum of correlation) (Meinhart *et al*., 2000). The ensemble correlation approach (PIV sum of correlation) is suitable for use when the SNR is very low and provides only average information of a set of instantaneous obtained in the recording. One way to evaluate the quality of velocity profile is to analyze the coherence of the target vector with its neighborhood. The coherence of time-averaged of V, Vx and Vy profiles with its neighborhood decreases from r/R= 1 to -1 and with the increasing of the flow (Fig. 6). The same behavior in relation to the measurement quality is observed in Fig. 6.

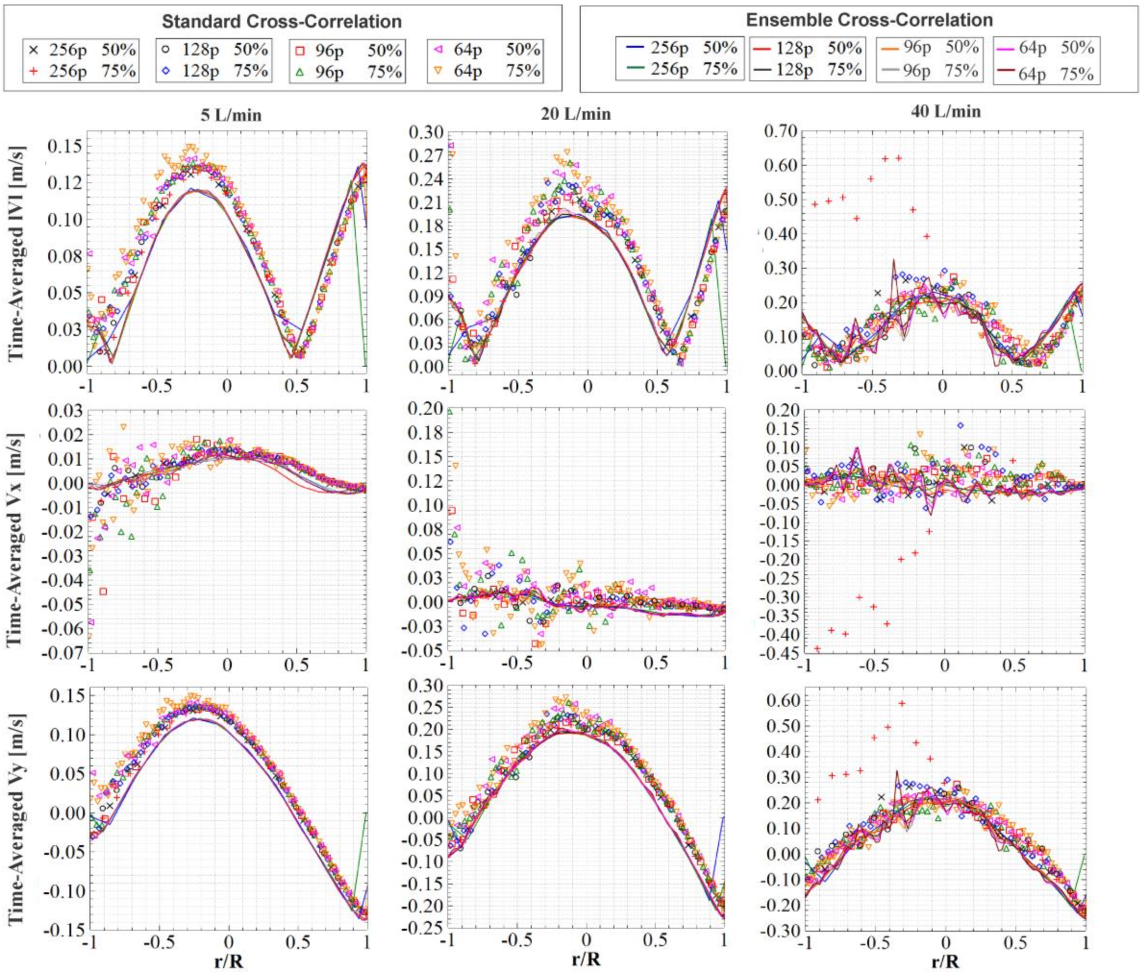

Figure 6. Distributions of time-averaged V, Vx and Vy along the radius at the axial position Y = 55.2 cm for flow rates of 5, 20 and 40 L / min using the standard cross-correlation and PIV ensemble correlation for different interrogation strategies (Tab 1).

The velocity profile obtained by the ensemble correlation approach showed greater consistency using eight interrogation strategies (except 64p 50% and 64p 75% for 40 L/min) demonstrating that the method is robust. Greater coherence between the standard and ensemble correlation approaches was obtained for interrogation strategy with interrogation window size of 256 pixels with 50% overlap. The dynamic velocity range (DVR) of the PIV technique is limited and may be an explanation for a greater discrepancy in of correlation peak detectability in the displacement in X direction than in Y direction. Because of the rising bubbles, the velocity in direction Y is larger than in X direction, facilitating the calculation of the displacement in Y. This problem can be solved using the pulses multiple recording approach by a time-resolved PIV system, which consists in systems with high frequency data acquisition. The out-of-plane movement can also have a significant effect on the velocity profile in the Fig. 6.

5. CONCLUSION

This work aims to assess the best PIV interrogation strategy in the investigation of the liquid phase velocity in a bubble column section using Fluorescent PIV. The distribution of time-averaged correlation coefficient, SNR and uncertainty were used as quality parameters of the interrogation strategy analyzed. The distributions of time-averaged velocities (modulus and components) were compared with the results obtained by the ensemble correlation. The gas flow rate used was 5, 20 and 40 L/min and 4000 pairs of images were recorded with a frequency of 4.2 Hz. Both distributions of time-averaged correlation coefficient and SNR decreased with increasing gas flow and with the final size of the interrogation window. Due to the presence of bubbles, which causes a non-homogeneous distribution of the laser light intensity in the field of view, it was observed that for the flow rate of 5 L/min the distribution of the time-averaged correlation coefficient decreased in the opposite region of the laser light emission. A decrease of correlation coefficient was observed in the column center for flow rates of 20 and 40 L/min. This fact can be explained by the presence of bubbles in front of the field of view, which compromises the recording of the particle images on the CCD sensor. It was also noticed that the distributions of time-averaged uncertainty increase from r/R = -1 to 1 for a flow rates of 5 L/min and 20 L/min (with a maximum at r/R = - 0.5) and they increases in the column center with 40 L/min. The coherence of time-averaged V, Vx and Vy profiles with its neighborhood decreases from r/R= 1 to -1 and with the increasing of the flow. The velocity profile obtained by the ensemble correlation approach showed greater consistency using eight interrogation strategies (except 64p 50% and 64p 75% for 40 L/min) demonstrating that the method is robust. The greatest coherence between the standard and ensemble correlation approach was obtained for interrogation window size of 256 pixels with 50% overlap.

6. ACKNOWLEDGEMENTS

The authors would like to acknowledge Petrobras and Capes for the financial support of this project

7. REFERENCES

Adrian, R. J. and Westerweel, J., 2011. Particle Image Velocimetry. Nova York: Cambridge University Press.

Keane, R.and Adrian, R., 1992. Theory of cross-correlation analysis of PIV images. Applied scientific research, Vol. 49, n. 3, p. 191-215.

Meinhart, C. D., Wereley, S. T. and Santiago, J.G., 2000. A PIV Algorithm For Estimating Time-Averaged Velocity Fields, Journal of Fluids Engineering, Vol. 122, p. 285-289.

Raffel, M.; Willert, C.; Wereley, S. T. and Kompenhans, J., 2007. Particle image velocimetry: a practical guide. Second Ed. Berlin Heidelberg: Springer Verlag.

Scarano, F. and Riethmuller, M.L., 2000. “Advances in iterative multigrid PIV image processing”, Experiments in Fluids [Suppl.], Vol.29, p. 51-60.

Westerweel, J. and Scarano, F., 2005. Universal outlier detection for PIV data. Experiments in Fluids, v. 39, n. 6, p. 1096-1100.

Wieneke, B., 2014. Generic a-posteriori uncertainty quantification for PIV vector fields by correlation statistics. 17th International Symposium on Applications of Laser Techniques to Fluid Mechanics, Lisbon, Portugal, 07-10 July.

Wieneke, B., Pfeiffer, K., 2010. “Adaptive PIV with variable interrogation window size and shape”, *15th Int Symp on Applications of Laser Techniques to Fluid Mechanics*, Lisbon, Portugal.

Wilson, J. F., Cobb, E. D., Kilpatrick, F.A., 1986. Fluorometric procedures for dye tracing. United States Government Printing. Washington.

Xue, Z., Charonko, J. J., Vlachos, P. P., 2013.Signal-to-noise ratio, error and uncertainty of PIV measurement. PIV13; 10th International Symposium on Particle Image Velocimetry, Delft, The Netherlands.

8. RESPONSIBILITY NOTICE

The authors Rodrigo de Lima Amaral, Diana Isabel Sánchez Forero, Guilherme José de Castilho, Sávio Souza Venâncio Vianna and Milton Mori are the only responsible for the printed material included in this paper.